Asian Journal of Nanoscience and Materials, 2018, 2(1), 49-65.

FULL PAPER

Host-guest interaction in chitosan– MX (3-chloro-4-(dichloromethyl)-5-hydroxy-2(5H)-furanone) complexes in water solution: Density Functional Study

Fatemeh Houshmand [a,b,*], Hamide Neckoudari[a] and Majid Baghdadi[c]

[a]*Department of Laboratory, Water and Wastewater quality control office, TPWW.Co. Tehran, Iran.*
[b]*Computational Physical Sciences Research Laboratory, School of Nano-Science, Institute for Research in Fundamental Sciences (IPM), P.O. Box 19395-5531 Tehran, Iran.*
[c]*Department of Environmental Engineering, Graduate Faculty of Environment, University of Tehran, Tehran, Iran.*

Received: 11 June 2018, Revised: 18 July 2018 and Accepted: 23 July 2018.

ABSTRACT: The present study is an attempt to provide an insight into the stability, in terms of interaction energy and thermodynamic parameter, and reactivity, quantified by reactivity descriptors, of the chitosan-MX and its analogous (EMX and ZMX) system. In this system a component is, MX (3-chloro-4-(dichloromethyl)-5-hydroxy-2(5H)-furanone) a mutagenic halogenated disinfection by products which are present in drinking water. In this sense, chitosan is an eco-friendly nano-adsorbent to remove oils, grease, heavy metalsand the fine particulate matter from water solution. Electronic and structural properties of chitosan during functionalization by metal were studied by density functional theory (DFT) calculations. Isolated and functionalized chitosan were optimized and their properties were evaluated. The results indicated that the properties of linking sites detect the most significant effects of functionalization process.

Degradation efficiency of MX and its analogous in water solvent and also the possibility of absorption of MX by chitosan nanoparticles in aqueous solution were studied via different level of theory.

KEYWORDS: Halogenated furanone (MX), MX analogous, Disinfection byproducts, Chitosan, Density functional theory.

GRAPHICAL ABSTRACT:

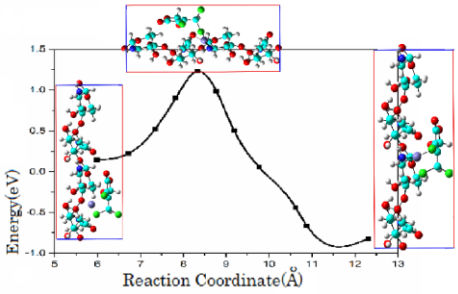

1. Introduction

During chlorine disinfection of drinking water, chlorine can react with natural organic matter (NOM) in raw water to generate halogenated disinfection

*Corresponding author: Fatemeh Houshmand, Email: fhooshmand@mail.kntu.ac.ir , Tel.: +98 21 22853649; fax: +98 21 22853650.

Asian Journal of Nanoscience and Materials

byproducts (DBPs). Halogenated furanone, a disinfection byproduct, present in chlorinated drinking water, is one of the most potent mutagens ever known. MX (3-chloro-4-(dichloromethyl)-5-hydroxy-2(5H)-furanone) is formed by the reaction of chlorine with complex natural organic matter. Its genotoxic effects are well documented [1–6]and these data indicate that MX induced thyroid and bile duct tumors [7].The mechanism by which MX exerts such an intense biological effect and interaction of them with nano-materials which are used in water treatment is still unclear.

MX is formed by the reaction of chlorine with complex organic matter in drinkingwater.Aromatic structures with an aldehyde group and substituents in the meta or para positions, e.g. like syringaldehyde or ferulic acid, can form MX upon chlorination [8], as can compounds, e.g. tryptophan, which can first form an aldehyde group [9]. It has been identified in drinking water MX which was found at mean concentrations ranging from 2 to 80 ng/ liter [6,10]. Registered by WHO, MX is one of the strongest bacterial mutagens ever tested, as highlighted by the Ames Salmonella typhimurium TA100 assay [8]. The observed mutagenic activity is significantly correlated only to the electrophilicity response of the ring forms [11]. However, analytical difficulties in measuring the low doses of MX encountered in drinking-water lead to uncertainty over whether this species would be genotoxic in vivo [12]. The World Health Organization (WHO) guidelines for drinking water maintain an updated register regarding MX, considering it unnecessary at present to propose a formal guideline value for MX in drinking water [13,14].

Chitosan (poly-β-(1→4)-2-amino-2-deoxy-D-glucose) is a naturalnitrogenous, amino-based, polysaccharide (Figure 2), which is produced in large quantities by N-deacetylation of chitin [13,15]. Marine crustaceans' shells are widely used as primary sources of chitin [16]. Chitosan , which is a biocompatible and biodegradable biopolymer is a liner and cationic polymer with numerous applications mainly dependent on presence of the amine group in its structure [17,18].

The adsorption process using chitosan, due to its effectiveness and cost effectiveness becomes an attractive remedial of effluents [19].The metal-chelating property of chitosan has beenmainly used in wastewater treatment. Recently, different metal chitosan complexes have been prepared to improve

Asian Journal of Nanoscience and Materials

its activity [20].Nanoparticles display unique physical and chemical features because of effects such as the quantum size effect, mini size effect, surface effect and

macro-quantum tunnel effect. Chitosan tripolyphosphate nanoparticles have been synthesized and mainly used as drug carrier as reported in previous studies [21].The major privilege of chitosan base absorption systems is the hydrophilicity combined with the polar groups, hydroxyl and also amine groups, which are capable to form long-range interaction with absorbent molecules [22]. Recently, some literature reports perceptive progress taking place with respect to a number of specialized chitosan derivatives envisaged to entangle some inherent restrictions of chitosan [23].

Dispersion-corrected DFT methods are endowed with very goodlevel of accuracy and have evolved as an alternative to methodsthat include extensive electron correlation in the calculation juxtaposed with a sufficiently large basis set [24,25]. Various dispersioncorrected functional are proposed and are being applied to assess strength of weak interactions such as hydrogen bonding. Amongthese DFT functional, several recent studies have outlined thesuitability of CAM-B3LYP for estimating strength of hydrogenbonding interaction [26,27].CAM-B3LYP combines the hybridqualities of Becke three parameter exchange and Lee, Yang andParr correlation functional (B3LYP) and the dispersion correctionessential for calculating interaction energy of hydrogen-bondedsystems [28,29].This functional was proven to yield much better result for exchange energy at large distances [30].

Herein, present study delves into the possibility of using chitosan nano-particles for absorbing MX from water solutions. Thermo-chemical parameters are calculated for clarifying the nature of interaction in Chitosan–MX system. Interaction energy, reactivity descriptors and electronic properties of this system are also utilized to describe the characteristics and features of interactions.

2. COMPUTATIONAL DETAILS

The ground-state calculations were performed for the isolated systems using a DFT approach, as implemented in the Quantum ESPRESSO package [31]. A plane wave basis set was used (50 Ry cutoff) with norm-conserving pseudopotentials and local-density approximation exchange correlation (XC) functional. The ground state structural

Asian Journal of Nanoscience and Materials

calculations such as mechanical properties and optical spectrum by DFT approach were performed by SIESTA package [ ]utilizing double-zeta polarized (DZP) basis set.After the evaluation of the active bonding sites for O and Cl atom (for MX and its analogous) and O and N atoms (in chitosan molecule) and its probablerecombination path, the next step was to find the activation energy along that path, so that kinetics of the recombination reaction could be predicted. An initial path was constructed and represented by a discrete set of images of the system connecting the initial and final states.To calculate the activation energy barrier,the nudged elasticband (NEB) [32] method implemented in the Quantum ESPRESSO package is used.

The ab-initio calculations were performed using the GAMESS US package [33].The calculations were performed within DFT using B3LYP (Becke three–parameter Lee–Yang–Parr) for exchange and correlation, which combines the hybrid exchange functional of Becke [34] with the correlation functional of Lee, Yang and Parr [35]. The calculations were performed with an extended 6– 311G(d,p) basis set. At the end of each geometry optimization a Hessian calculation was conducted to guarantee that the final structure corresponds to a true minimum, using the same level of theory as in the geometry optimization. For the optimized geometries of the studied structures, single-point energy calculations were performed with the conditions mentioned above (B3LYP functional and 6-311G(d,p) basis set). All studied structures were also optimized using the Polarizable Continuum Model (PCM) with the solvent water, using the same level of theory as in previous calculations.

Simulations were performed by using LAMMPS (large-scale atomic/molecular massively parallel simulator) open-source classical MD code [36]. Periodic boundary conditions were imposed in all directions of simulation cells.After the structure optimization, the system is thermalized using NVT ensemble for 1ns where the temperature fluctuation is minimized to be around 5 K. The simulation system is then switched to NVE ensemble to run for 10 ns. Non-bonded interactions were truncated at 10 Å cutoff distance and the long-range electrostatic interactions were predicted using particle-particle particle-mesh method [37]. Newton’s equation of motion was solved with velocity Verlet integrator using a time step of 0.5 fs [38]. During simulations, temperature and pressure were

Asian Journal of Nanoscience and Materials

controlled via Nose-Hoover algorithm as thermostat and barostat [39].

3. RESULTS AND DISCUSSION

I. Structural properties

It is known [40]that MX(C5H3Cl3O3) can predominate as a halogenated hydroxyfuranonesring (HHF) and the open-ring form 2-chloro-3-(dichloromethyl)-4-oxobutenoic acid tautomer ((E) and (Z) ,Figure 1)in respect to the acidity of solution. Thering form exists in solutions with pH<5.5, whereasthe Z-open form will be present at standard pH of drinking-water [41].

To investigate the interaction of MX analogous with chitosan,the fully optimized structure of MX, EMX and ZMX were obtained by geometry optimization(Figure1).

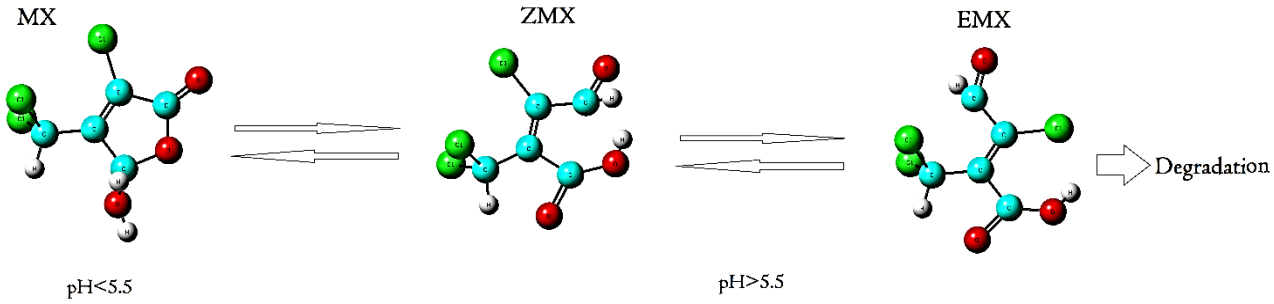

Fig. 1. Optimized structure of different form of MXin different range of pH.

Structural parameters and partial charge on different atoms for MX and studied analogous are listed in Table 1. According to Table 1, partial charge on halogen atoms are more negative in MX analogous. In case of partial charge on Oxygen atoms, MX and ZMX are approximately the same and for EMX charge of Oxygen atoms are more positive than other. The electrostatic term of total energy is nearly the same and for MX is more negative.

Figure 2, illustrates the density of state for MX and its analogous. The Fermi level of energy population in case of EMX is near to zero. Although the Fermi level have population in MX and ZMX none of the have not a considerable amount at this level of energy.

Asian Journal of Nanoscience and Materials

Table 1. Total energy (eV), Electrostatic energy (eV), bader charges for MX and their analogous.

	$E_{tot}(eV)$	E_{elec}	*Bader Charge*
MX	-3446.25	-4534.31	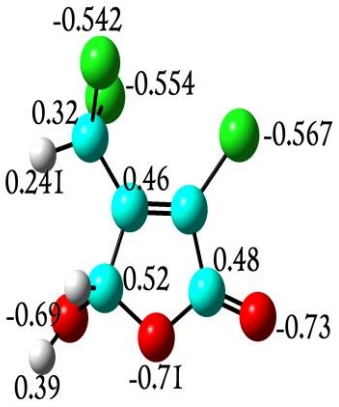
ZMX	-3506.96	-4480.92	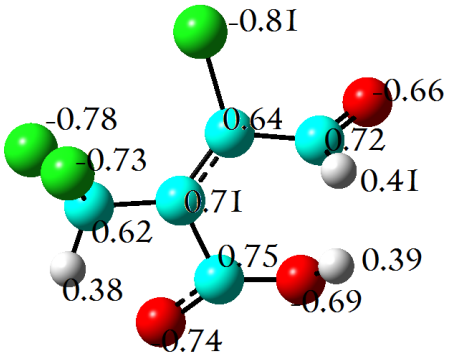
EMX	-3508.77	-4492.65	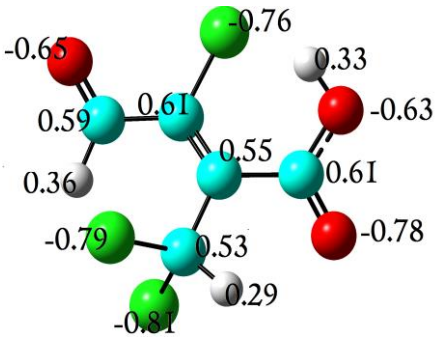

Asian Journal of Nanoscience and Materials

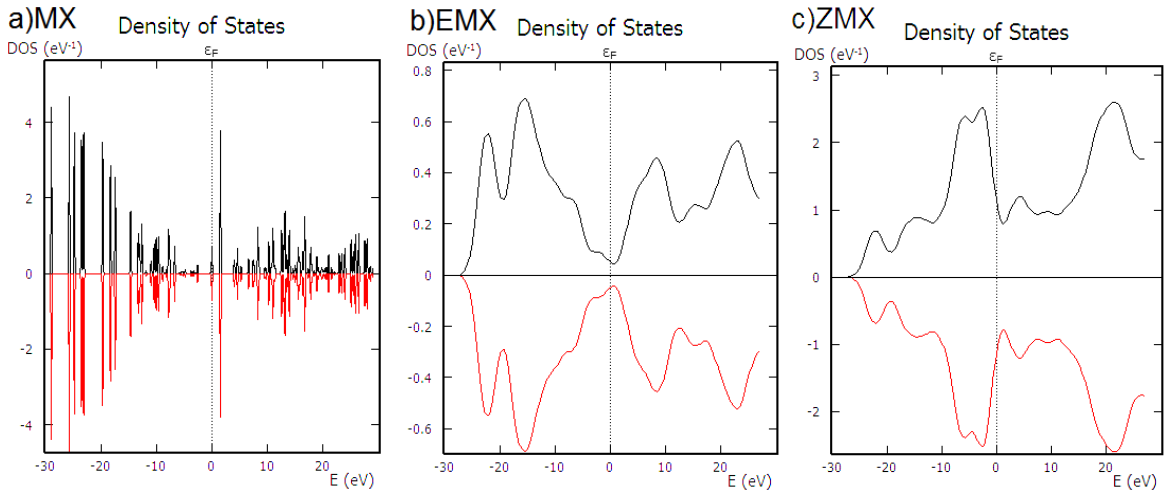

Fig. 1. Density of states for (a) MX (b) EMX (c)ZMX. Dash lines represent the position of the Fermi level.Upper and lower panels are for spin-up and spin-down states respectively and the Fermi level is at zero energy.

As clearly obvious in DOS of EMX the level of energies near to fermi level are unoccupied. Density of states diagram for MX molecule demonstrate a very sharp peaks in contrast to EMX and ZMX diagrams. It may be referring to long range interactions in these recent molecules which is not considered in DFT calculation. Spin-up and down states in all case are coincides which indicate that in none of studied halogenated furanone we have not spin-polarization.

Angular distribution for MX and its analogous are illustrated in respect to C3 as the center,Figure 3.

Using the above mentioned optimized geometries for Fe absorbed chitosan and MX (and its analogous), the interaction energies of the adducts are calculated as the following equation:

$$E_{int} = E_{AB/C} - E_{A/C} - E_B + E_{bsse}$$

Herein, the correction term, E_bsse, is the basis set superposition error which included to overcome the effect of basis set incompleteness at CAM-B3LYP/6-31++G(d,p) level of theory(Table 2).

Regarding the hydrolysis energy and interaction energy of chitosan in solvent, it is obvious that active points on chitosan structure under alkaline condition are strongly protonated. According to [42], free amino groups of chitosan cannot be protonated in low concentration of proton so only the hydroxyl groups can capture the proton from aqueous media. In contrast, Fe absorbed chitosan in low concentration of

Asian Journal of Nanoscience and Materials

proton have an obviously high interaction with MX(Table 2).

Results indicate that the interaction ion energy of chitosan-MX system in gas phase is more than the interaction energy in solvent. It may be referring to protonation of amine group in solution which prevents the interaction between amine group and MX.

Table2. compares calculated difference activation parameters for studied systems. Activation entropies for functionalized chitosan coupled with ZMX (ZMX-Chitosan/Fe(0)) are quite high and even positive in EMX/functionalized chitosan system where small negative values would be expected.

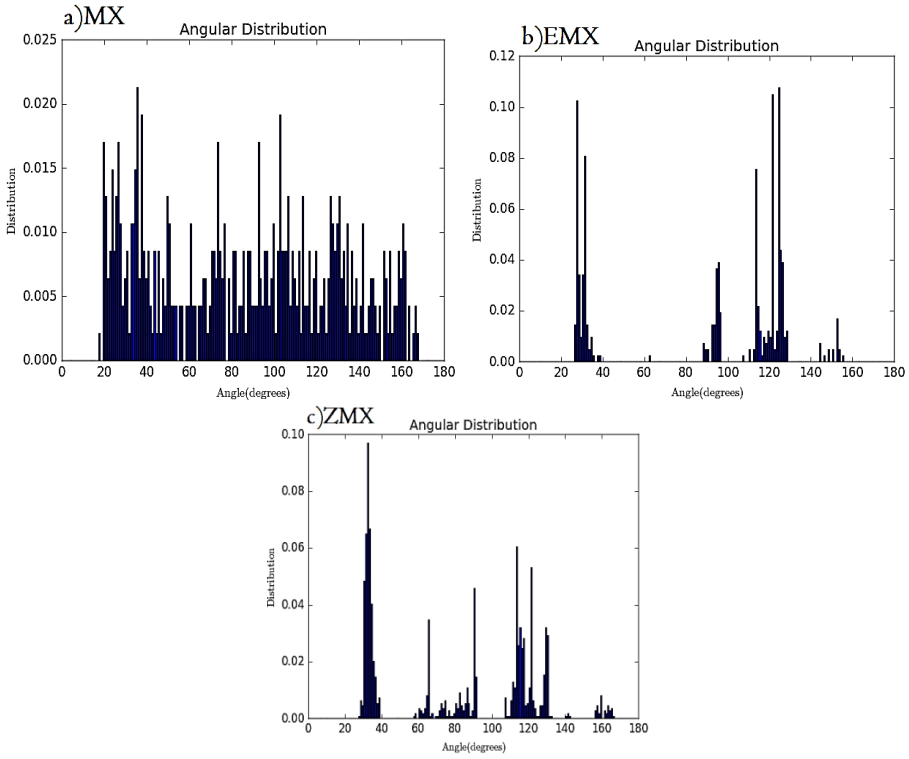

Fig.2. Angular distribution for MX,EMX,ZMX

As regards to the Table 2 results, ZMX/Chitosan is very close in activation energy to the ZMX/Chitosan. The neutral rate constant for hydrolysis/decomposition reaction is equal to 2.7× 〖10〗 ^(-4)min (calculated by nudged elastic band approach) for MX –chitosan hydrolysis other case are approximately similar.

The reported values in Table2 show that EMX and ZMX activation enthalpies are obviously similar, So the activation

Asian Journal of Nanoscience and Materials

entropies for these two forms of MX are null. In case of MX-Chitosan, activation entropy is slightly positive. These results are approximately in accordance to the expected results for a ring-opening reaction which occur f or an uni-molecular system. Negative activation entropies for chitosan-heavy metal system suggest a decrease in thickness of hydration shell around system.

Table 1. Calculated energy barriers for the hydrolysis of studied systems and bsse corrected interaction energy values in vacuum and in water solution.

	$\Delta^{\ddagger}H^{\ominus}$*(Kj/mol)*	$\Delta^{\ddagger}S^{\ominus}$*(Kj/mol)*	$\Delta^{\ddagger}G^{\ominus}$*(Kj/mol)*	$\triangle E_{int}$*(water)*	$\triangle E_{int}$*(gas)*
MX	69	-115	109	-	-
EMX	55	-91	93	-	-
ZMX	43	-108	97	-	-
Chitosan	21	-193	192	-	-
MX-Chitosan	36	-207	169	-22.08	-46.10
MX-Chitosan/Fe(0)	31	-153	175	-39.91	-51.87
EMX-Chitosan	41	-108	225	-17.99	-18.33
EMX-Chitosan/Fe(0)	39	95	214	-17.56	-18.47
ZMX-Chitosan	38	-109	221	-19.14	-20.01
ZMX-Chitosan/Fe(0)	32	-103	182	-20.55	-2.89

According to

Table ***12***,hydrolysis of individual chlorinated furanone in aqueous media is very slow.

Detection and measurement of observed concentration of MX (2-80 ng/lit) in drinking water because of the complex sample composition and matrix constituents present in concentrated water samples and also, because of the complex fragmentation pattern of MX have intrinsic difficulties

Asian Journal of Nanoscience and Materials

[43]. According to EPA guideline measuring MX by GC-ECD requireshigh volume of MTBE as solvent which is hazardous to the environment [43]. On the other hand, level of recovery and uncertainty of all of existing measuring methods for detection of MX are low [44]. The green nanostructures in some cases [45] can ramp the precision of detection.

Chitosan ($C_{56}H_{103}N_9O_{39}$) is a linear polysaccharide composed of randomly distributed beta ($\beta_1$to 4)linked D-glucosamine(GlcN unit), and N-Acetyl-D-glucosamine (NAGunit).

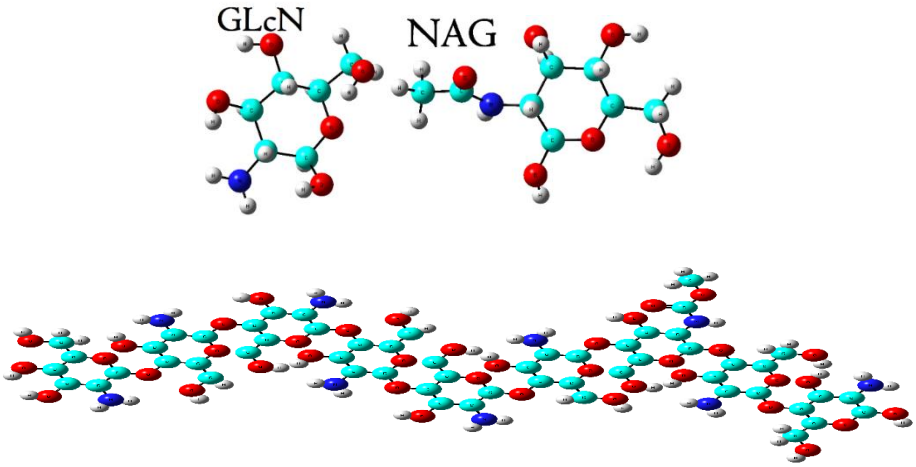

Fig. 3. Optimized structure of chitosan(GLcN-NAG) and its units.

The structural parameters of MX/Chitosan systemwere obtained by DFT study and are listed in Table1.We typically set the structural optimization method to allow variable cell relaxation for MX/Chitosan system. The unit cell of MX/Chitosan systemis slightly expanded with respect to Chitosan's cell.We studied 1:1 concentration of MX and its analogous adsorbed on Chitosan.

Table 2. Structural parameters. Chemical Potential$^{\mu}$,

		$\alpha(X-N-C)$ $(\alpha(X-O-C))$	d_{C-X}	d_{O-X}	d_{N-X}	E_{coh} *(eV/atom)*	$\mu(eV)$	E_a *(eV)*
Pure	**MX**	89(120)	1/37	-	-	25/31	-1/97	-

Asian Journal of Nanoscience and Materials

	EMX	87(131)	1/73			19/60	-4.77	-
	ZMX	87(136)	1/42	--	--	7/24	-4.71	-
	Chitosan	-	--			5/12	-0.45	-
Complex	**MX-Chitosan**	83(91)	1/37	1.50	1.31	3/29	0.39	-1/91
	MX-Chitosan/Fe(0)	85(32)	1/72	1/51	1.41	6/98	1.13	2/36
	EMX-Chitosan	89(120)	1/74	1⁄45	1.30	1.31	0.12	-1/91
	EMX-Chitosan/Fe(0)	87(131)	1.52	1⁄45	1.32	1.72	0.15	2/36
	ZMX-Chitosan	92(141)	1.36	1⁄44	1.33	2.03	0.18	-1/91
	ZMX-Chitosan/Fe(0)	89(136)	1.40	1⁄45	1.31	2.86	0.24	2/36

Fig. ***45***illustrates the density of states for chitosan/MX system (a) which indicates that the level of energy near to fermi level of energy are unoccupied. Spin-resolved density of states indicates that chitosan/MX is not spin-polarized. On the other hand, chitosan(Fe)/MX system shows an obvious spin-polarization specially in minority spin near to fermi level of energy.

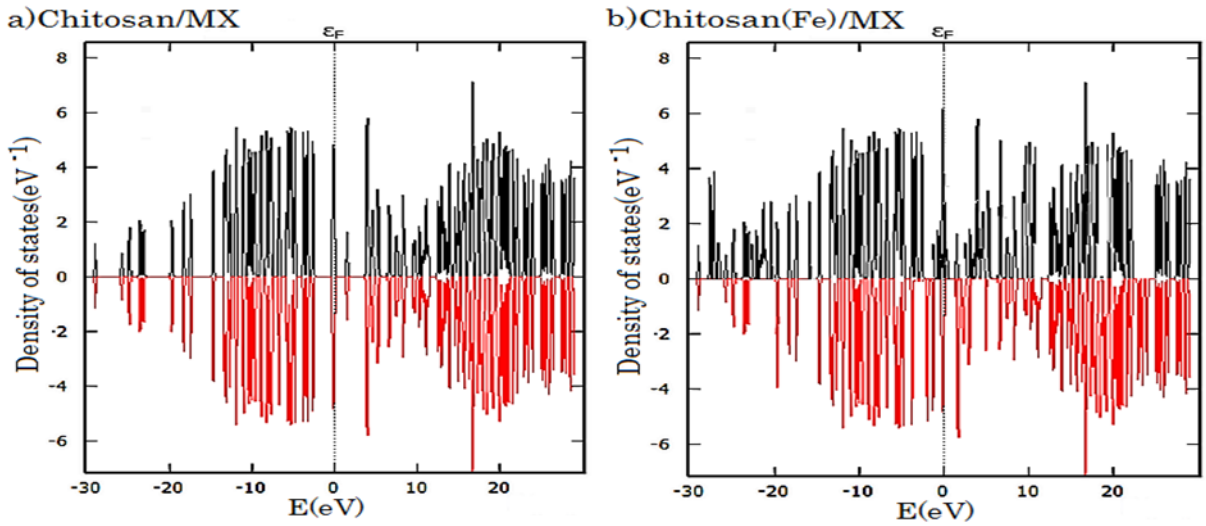

Fig. 4. Density of states for (a) Chitosan/MX (b) Chitosan(Fe)/MX. Dash lines represent the position of the Fermi level.Upper and lower panels are for spin-up and spin-down states respectively and the Fermi level is at zero energy.

To calculate the activation energy barrier, the nudged elastic band (NEB) method implemented in the Quantum ESPRESSO package is used. Result of activation energy for reaction between Fe atom and chitosan supercell indicates that the process is exothermic reaction.

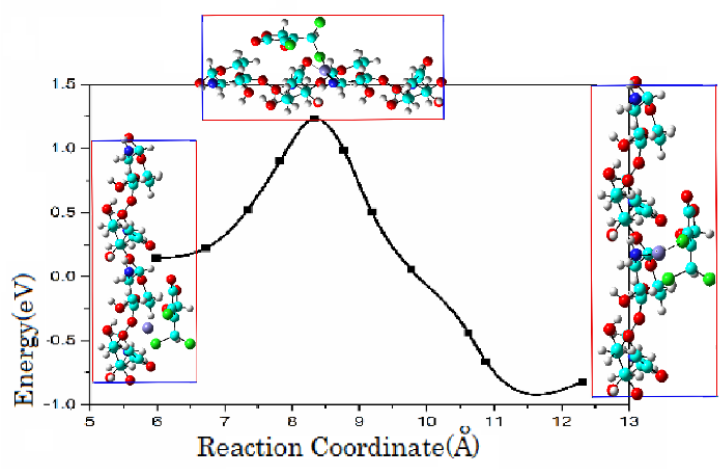

Fig. 5. Calculated energy profile involved in the adsorption of MX on Chitosan(Fe). The optimized structures ofinitial, excited state and final images along the energy path are also plotted in the inset.

I. Dynamics Modelling

At the beginning of MD simulation, the atom position and lattice constants of MX are adjusted using conjugate gradient algorithm until the potential energy of the system is minimized. This structure optimization step in MD simulations is performed to make sure that the atoms are at the equilibrium positions in MD simulations, because the potential field developed does not perfectly match the energy surface from DFT calculation due to the limitation of the functional forms assigned [46]. As expected, the lattice constants are slightly changed after the MD structure optimization. To investigate the local structure of MX/Chitosan system in water solution as a function of operating temperature the radial distribution function (RDF) was used. RDF shows the probability distribution of imolecule around reference jmolecule, and is defined as equation (1):

$$g_{i-j}(r) = \frac{\left(\frac{n_j}{4\pi r^2 \Delta r}\right)}{\left(\frac{N_j}{V}\right)} \qquad (1)$$

where $n_j$is the number of j atoms located around imolecule inside a spherical shell of thickness Δr, N_j is the total number of j molecule employed when constructing simulation cell and V is the equilibrated cell volume.

Asian Journal of Nanoscience and Materials

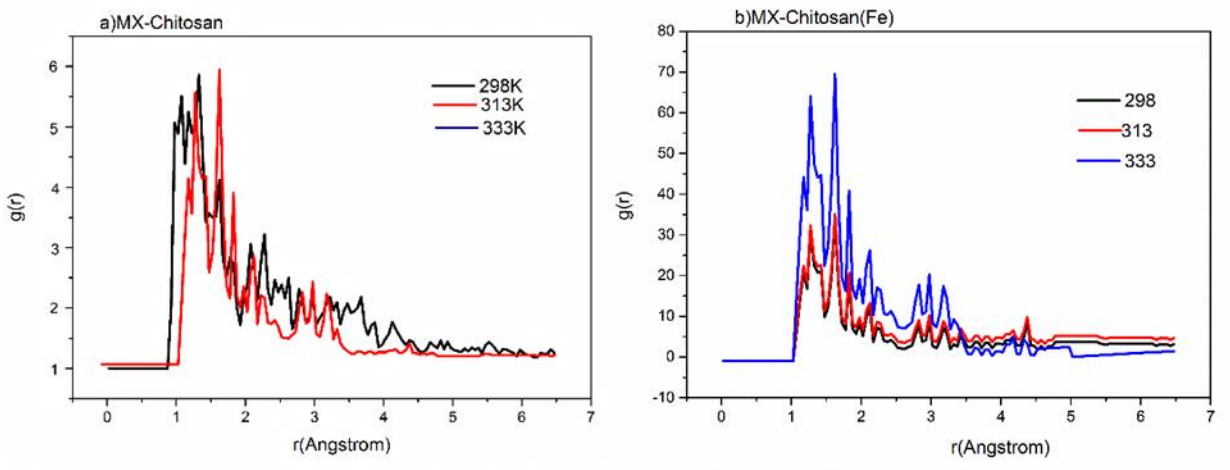

Fig. 6. Radial Distribution function for Cl(MX)-N(chitosan).

Dynamic property of hydrated MX-chitosan system under varied operating temperatures wasexplored by means of the diffusion coefficients (D) for amino groups, water moleculesand hydronium ions. Diffusivity was calculated (Table ***34***)using the slopeof mean squared displacement (MSD) or Einstein relation according to the following equation(2):

$$D = \frac{1}{6}\lim_{t\to\infty}\frac{dMSD(t)}{dt} = \frac{1}{6N}\lim_{t\to\infty}\frac{d}{dt}\sum_{j=1}^{N}\left[\left(r_j(t) - r_j(0)\right)^2\right] \quad (2)$$

where N is the total number of j atoms (here, halide atoms, oxygenatoms for hydroxyl group or hydronium ions), r_j (t) and r_j (0) are the positions for j atoms attime t and at the beginning of production MD simulations, respectively. It should be noted thediffusivity for hydroxyl group and hydronium ion was computed using both hydrogen and oxygen atomsand the results were the same.

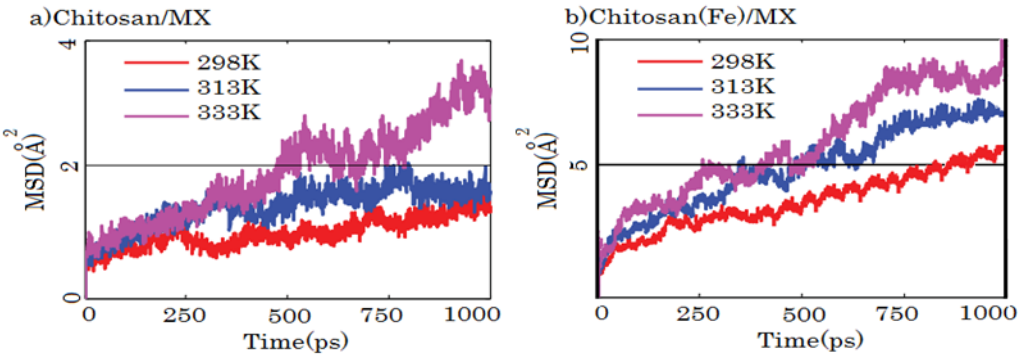

Fig.7. Mean squared displacement of halide atom (MX) at temperature 298,313,333K for (a) chitosan/MX system and (b) Chitosan(Fe)/MX.

Figure 4 indicates the mobility of halide group in terms of mean squared displacementof halogen atom on chitosan layer for different temperatures. It is

Asian Journal of Nanoscience and Materials

obvious that halide groups demonstrate increased dynamics at highertemperatures which is attributed to increased kinetic energy of such groups at increasedtemperatures.

Table 3. Diffusion coefficients of halide, hydroxyl group of MX and hydronium ion at 298,313 and 333K on Chitosan polymer.

Temperature(K)	**D× $10^{-3}(cm^2/s)$**		
	Cl^-	OH^-	H_3O^+
298	0.0045	0.09	0.068
313	0.0072	0.06	0.058
333	0.0091	0.02	0.036

Furthermore MSD of both hydronium ions and water molecules enhances as the temperature is increased. Therefore, increasing the temperature enables hydronium ions and hydroxyl group to migrate more quickly within the solvated morphology of aromatic MX. The molecular dynamics estimated diffusion coefficients for halide ion, hydronium ions and hydroxyl group were listed in Table ***34*** and Table ***45*** for chitosan and metal absorbed chitosan respectively. It is generally accepted and remarkable to mention here that the amino groups of chitosan are responsible for its complexing with metal ions as the cations have a preference to ligands with the amino groups [47]. It can be seen that all calculateddiffusivities exhibit an increasing trend against temperature. Halide ion has the leastdiffusion coefficient values due to the fact that in contrast to the hydronium ions and hydroxyl group on MX they are attached to only the amine group of chitosan structure. When Fe atom absorbed on chitosan, chelating metal on amine with MX cause higher diffusion of halide ion on chitosan.

In addition, it is obvious that the hydronium ion diffusion coefficient is higher than that of hydroxyl since the calculation of diffusivity of hydronium ion only includes the vehicular component of the interfacial diffusivities of hydronium ions.

Asian Journal of Nanoscience and Materials

Table 4. Diffusion coefficients of halide, hydroxyl group of MX and hydronium ion at 298,313 and 333K on metal absorbed Chitosan polymer.

Temprature(K)	**D× $10^{-3}(cm^2/s)$**		
	Cl^-	OH^-	H_3O^+
298	0.0054	0.08	0.068
313	0.0083	0.06	0.058
333	0.0102	0.02	0.036

II. Reactivity

From among several reactivity descriptors defined by DFRT, energy of highest occupied molecular orbital, global hardness, chemical potential and electrophilicity are considered for analysis of reactivity of the title systems in the present study. Global hardness (g) is the second derivatives of energy with respect to the number of electrons [48] The working formula of g, as derived from finite difference approximation and Koopmans' theorem [49,50]: $\eta = (E_{LUMO} - E_{HOMO})/2$, where, E_{HOMO} is the energy of the highest occupied molecular orbital (HOMO) and E_{LUMO} is the energy of the lowest unoccupied molecular orbital (LUMO). Electrophilicity (x) [36] is expressed as$\omega = (\frac{\mu^2}{2\eta})$, where $\mu$is called chemical potential and$\mu = (E_{LUMO} + E_{HOMO})/2$.Extensions of the electrophilicity into theframework of a spin-polarized version of DFT have alsobeen introduced in order to properly describe both charge-transfer and spin-polarization processes.

Among the reactivity descriptors, HOMO energy (E_{HOMO}), global hardness (g) and chemical potential (μ) are important from the viewpoint of chemical stability of a system. Variations of these parameters

Table ***56***.

Table 5. Gas phase reactivity parameters (in kcal/mol) of chitosan, chitosan-Fe, chitosan/chitosan-Fe-MX adducts at M06-2X/6-31++G (d,p) level of theory.

	E_{HOMO}	η	μ	ω
MX	-291.94	106.18	-185.76	162.49
Chitosan	-175.87	71.08	-69.37	59.87

Chitosan-Fe	-179.95	77.13	-95.01	109.25
Chitosan@MX	-311.99	88.47	-223.52	282.35
Chitosan-Fe@MX	-319.79	77.24	-242.56	380.85

Measurement of E_{HOMO} of a species is an important factor because it measures the electron donating ability i.e. the reactivity of the species. A sharp drop of HOMO energy in MX upon adduct formation with the Chitosan/Chitosan-Fe is observed which advocates a more stable HOMO in adducts than in bare MX. This result predicts that Chitosan/Chitosan-Fe @MX adducts are less prone to attack by any electrophile than bare MX. Similarly, more negative value of μ signifies relatively greater stability of the system. As it is evident from Table 3 in line with E_{HOMO}, chemical potential data also portrays greater chemical stability of Chitosan/Chitosan-Fe @MX adducts than bare MX.

4. Conclusions

In conclusion, the electronic and structural properties of a MX-analogous/chitosan and have been studied. Adsorption of TM can effectively modulate the structural and electrical properties of these structures. Adding metal to MX-analogous complex with chitosan obviously can tunes the stability of complex. Active site for binding each analogous with matal and also with chitosan have been determined. Calculation thermodinamics parameters of hydrolysis of studied structures in water solution shows that metal absorbed systems are more stable species in water solution comparing other. The HOMO level of energy for prinstin chitosan and MX system compare to MX/chitosan or MX/chitosan(Fe) indicates that complex systems are more stable than pure systems.

5. Acknowledgments

The authorsare grateful to School of Computer Science, Institute for Research in Fundamental Science (IPM), Tehran, Iran, for professional technical assistance.F.H also deeply appreciatesQE developers for very useful discussions.This research was enabled in part by support provided by WestGrid (www.westgrid.ca) and Compute

Canada Calcul Canada (www.computecanada.ca).

Refrences:

1. G. Brunborg, J.A. Holme, E.J. Søderlund, and E. Dybing, (**1990**) *Prog. Clin. Biol. Res.*, **340**:43 .
2. G. Brunborg, J.A. Holme, E.J. Søderlund, J.K. Hongslo, T. Vartiainen, S. Lötjönen, and G. Becher, (**1991**) *Mutat. Res. Toxicol.*, **260**:55–64 .
3. U.K. COM, (**n.d.**) .
4. F.B. Daniel, M. Robinson, G.R. Olson, J.A. Stober, and N.P. Page, (**1994**) *Journal-American Water Work. Assoc.*, **86**:103–111 .
5. K. Heiskanen, P. Lindström-Seppö, L. Haataja, S.-L. Vaittinen, T. Vartiainen, and H. Komulainen, (**1995**) *Toxicology*, **100**:121–128 .
6. B. Holmbom, R.H. Voss, R.D. Mortimer, and A. Wong, (**1984**) *Environ. Sci. Technol.*, **18**:333–337 .
7. H. Komulainen, S.-L. Vaittinen, T. Vartiainen, J. Tuomisto, V.-M. Kosma, E. Kaliste-Korhonen, S. Lötjönen, and R. K. Tuominen, (**1997**) *J. Natl. Cancer Inst.*, **89**:848–856 .
8. H. Horth, J.K. Fawell, C.P. James, and W.F. Young, The fate of the chlorination-derived mutagen MX in vivo, in: Rep. No. FR025 Found. Water Res., Alien House Marlow Bucks, England, (1991).
9. Z. Huixian, L. Junhe, C. Zhuo, Y. Chengyong, Z. Jinqi, and Z. Wen, (**2000**) *Water Res.*, **34**:225–229 .
10. J. Hemming, B. Holmbom, M. Reunanen, and L. Kronberg, (**1986**) *Chemosphere*, **15**:549–556 .
11. H. Huuskonen, R. Venäläinen, and H. Komulainen, (**2003**) *Birth Defects Res. Part B Dev. Reprod. Toxicol.*, **68**:172–179 .
12. B. Li, C.-L. Shan, Q. Zhou, Y. Fang, Y.-L. Wang, F. Xu, L.-R. Han, M. Ibrahim, L.-B. Guo, and G.-L. Xie, (**2013**) *Mar. Drugs*, **11**:1534–1552 .
13. E. Rincon, F. Zuloaga, and E. Chamorro, (**2013**) *J. Mol. Model.*, **19**:2573–2582 .
14. J.R. Meier, A.B. DeAngelo, F.B. Daniel, K.M. Schenck, J.U. Doerger, L.W. Chang, F.C. Kopfler, M. Robinson, and H.P. Ringhand, Genotoxic and carcinogenic properties of chlorinated furanones: important by-products of water chlorination, in: Genet. Toxicol. Complex Mix., Springer, (1990), pp. 185–195.
15. F. Edition, (**2011**) *WHO Chron.*,

38:104–108 .

16. M. Rinaudo, (**2006**) *Prog. Polym. Sci.*, **31**:603–632 .
17. J. Zhang, W. Xia, P. Liu, Q. Cheng, T. Tahi, W. Gu, and B. Li, (**2010**) *Mar. Drugs*, **8**:1962–1987 .
18. I. Younes and M. Rinaudo, (**2015**) *Mar. Drugs*, **13**:1133–1174 .
19. B. Bellich, I. D'Agostino, S. Semeraro, A. Gamini, and A. Cesàro, (**2016**) *Mar. Drugs*, **14**:99 .
20. C. Cook and V.G. Gude, Characteristics of Chitosan Nanoparticles for Water and Wastewater Treatment: Chitosan for Water Treatment, in: Adv. Nanomater. Water Eng. Treat. Hydraul., IGI Global, (2017), pp. 223–261.
21. W. Chooaksorn and R. Nitisoravut, Heavy metal removal from aqueous solutions by chitosan coated ceramic membrane, in: Proc. 4th Int. Conf. Informatics, Environ. Energy Appl. Pattaya, Thail., (2015), pp. 28–29.
22. W.-L. Du, S.-S. Niu, Y.-L. Xu, Z.-R. Xu, and C.-L. Fan, (**2009**) *Carbohydr. Polym.*, **75**:385–389 .
23. A.M. De Campos, A. Sánchez, and M.J. Alonso, (**2001**) *Int. J. Pharm.*, **224**:159–168 .
24. T. Kean, S. Roth, and M. Thanou, (**2005**) *J. Control. Release*, **103**:643–653 .
25. M. Prabaharan and A. Tiwari, (**2010**) *Chitin, Chitosan, Oligosaccharides Their Deriv. Biol. Act. Appl.*, 173 .
26. S. Grimme, (**2010**) *J. Chem. Phys.*, **132**:154104 .
27. E. Torres and G.A. DiLabio, (**2012**) *J. Phys. Chem. Lett.*, **3**:1738–1744 .
28. M. Soniat, D.M. Rogers, and S.B. Rempe, (**2015**) *J. Chem. Theory Comput.*, **11**:2958–2967 .
29. G.A. DiLabio, E.R. Johnson, and A. Otero-de-la-Roza, (**2013**) *Phys. Chem. Chem. Phys.*, **15**:12821–12828 .
30. A.D. Becke, (**1993**) *J. Chem. Phys.*, **98**:5648–5652 .
31. P. Giannozzi, S. Baroni, N. Bonini, M. Calandra, R. Car, C. Cavazzoni, D. Ceresoli, G.L. Chiarotti, M. Cococcioni, and I. Dabo, (**2009**) *J. Phys. Condens. Matter*, **21**:395502 .
32. J.M. Soler, E. Artacho, J.D. Gale, A. García, J. Junquera, P. Ordejón, and D. Sánchez-Portal, (**2002**) *J. Phys. Condens. Matter*, **14**:2745 .
33. G. Henkelman and H. Jónsson, (**2000**) *J. Chem. Phys.*, **113**:9978–9985 .

34. M.W. Schmidt, K.K. Baldridge, J.A. Boatz, S.T. Elbert, M.S. Gordon, J.H. Jensen, S. Koseki, N. Matsunaga, K.A. Nguyen, and S. Su, (**1993**) *J. Comput. Chem.*, **14**:1347–1363 .
35. A.D. Becke, (**1988**) *Phys. Rev. A*, **38**:3098 .
36. C. Lee, W. Yang, and R.G. Parr, (**1988**) *Phys. Rev. B*, **37**:785 .
37. S. Plimpton, (**1995**) *J. Comput. Phys.*, **117**:1–19 .
38. M. Deserno and C. Holm, (**1998**) *J. Chem. Phys.*, **109**:7694–7701 .
39. R.G. Parr and R.G. Pearson, (**1983**) *J. Am. Chem. Soc.*, **105**:7512–7516 .
40. R.G. Parr, R.A. Donnelly, M. Levy, and W.E. Palke, (**1978**) *J. Chem. Phys.*, **68**:3801–3807 .
41. S.D. Richardson, M.J. Plewa, E.D. Wagner, R. Schoeny, and D.M. DeMarini, (**2007**) *Mutat. Res. Mutat. Res.*, **636**:178–242 .
42. N. Suzuki and J. Nakanishi, (**1995**) *Chemosphere*, **30**:1557–1564 .
43. M. Gonsior, P. Schmitt-Kopplin, H. Stavklint, S.D. Richardson, N. Hertkorn, and D. Bastviken, (**2014**) *Environ. Sci. Technol.*, **48**:12714–12722 .
44. P. Andrzejewski and J. Nawrocki, (**2005**) *Glob. NEST J.*, **7**:27–42 .
45. X. Qian, X. Gu, and R. Yang, (**2015**) *J. Phys. Chem. C*, **119**:28300–28308 .
46. I. Onoka, A. Pogrebnoi, and T. Pogrebnaya, (**2014**) *Int. J. Mater. Sci. Appl.*, **3**:121–128 .
47. S. Mao, W. Sun, and T. Kissel, (**2010**) *Adv. Drug Deliv. Rev.*, **62**:12–27 .
48. T. Koopmans, (**1934**) *Physica*, **1**:104–113 .
49. R.G. Parr, L. v Szentpaly, and S. Liu, (**1999**) *J. Am. Chem. Soc.*, **121**:1922–1924 .
50. P. Geerlings, F. De Proft, and W. Langenaeker, (**2003**) *Chem. Rev.*, **103**:1793–1874 .

How to cite this manuscript: Fatemeh Houshmand *, Hamide Neckoudari and Majid Baghdadi. Host-guest interaction in chitosan– MX (3-chloro-4-(dichloromethyl)-5-hydroxy-2(5H)-furanone) complexes in water solution: Density Functional Study. Asian Journal of Nanoscience and Materials, 2018, **2**(1) , 49-67.